
Article:
Yajzey, R., Bentley, M. A. orcid.org/0000-0001-8401-3455, Simpson, E. C. et al. (22 more authors) (2021) Spectroscopy of the T = 2 mirror nuclei 48Fe/48Ti using mirrored knockout reactions. Physics Letters, Section B: Nuclear, Elementary Particle and High-Energy Physics. 136757. ISSN 0370-2693

https://doi.org/10.1016/j.physletb.2021.136757

Physics Letters B 823 (2021) 136757

Contents lists available at ScienceDirect

Physics Letters B

www.elsevier.com/locate/physletb

Spectroscopy of the $T = 2$ mirror nuclei ^{48}Fe/^{48}Ti using mirrored knockout reactions

R. Yajzey [a,b,*], M.A. Bentley [a,*], E.C. Simpson [c], T. Haylett [a], S. Uthayakumaar [a], D. Bazin [d,e], J. Belarge [d], P.C. Bender [d], P.J. Davies [a], B. Elman [d,e], A. Gade [d,e], H. Iwasaki [d,e], D. Kahl [f,j], N. Kobayashi [d], S.M. Lenzi [i], B. Longfellow [d,e], S.J. Lonsdale [f], E. Lunderberg [d,e], L. Morris [a], D.R. Napoli [g], X. Pereira-Lopez [a], F. Recchia [d,i], J.A. Tostevin [h], R. Wadsworth [a], D. Weisshaar [d]

[a] Department of Physics, University of York, Heslington, York YO10 5DD, United Kingdom
[b] Department of Physics, Faculty of Science, Jazan University, Jazan 45142, Saudi Arabia
[c] Research School of Physics, The Australian National University, Canberra ACT 2600, Australia
[d] National Superconducting Cyclotron Laboratory, Michigan State University, East Lansing, MI 48824, USA
[e] Department of Physics and Astronomy, Michigan State University, East Lansing, MI 48824, USA
[f] School of Physics and Astronomy, University of Edinburgh, Edinburgh EH9 3FD, United Kingdom
[g] INFN, Laboratori Nazionali di Legnaro, I-35020 Legnaro, Italy
[h] Department of Physics, Faculty of Engineering and Physical Sciences, University of Surrey, Guildford, Surrey GU2 7XH, United Kingdom
[i] Dipartimento di Fisica e Astronomia dell'Università and INFN, Sezione di Padova, I-35131 Padova, Italy
[j] Extreme Light Infrastructure – Nuclear Physics, Horia Hulubei National Institute for R&D in Physics and Nuclear Engineering (IFIN-HH), 077125 Bucharest-Măgurele, Romania

ARTICLE INFO

Article history:
Received 18 June 2021
Received in revised form 26 August 2021
Accepted 24 October 2021
Available online 29 October 2021
Editor: B. Blank

ABSTRACT

A sequence of excited states has been established for the first time in the proton-rich nucleus ^{48}Fe (Z=26, N=22). The technique of mirrored (i.e. analogue) one-nucleon knockout reactions was applied, in which the $T_z = \pm 2$ mirror pair, ^{48}Fe/^{48}Ti were populated via one-neutron/one-proton knockout from the secondary beams ^{49}Fe/^{49}V, respectively. The analogue properties of the reactions were used to help establish the new level scheme of ^{48}Fe. The inclusive and exclusive cross sections were determined for the populated states. Large differences between the cross sections for the two mirrored reactions were observed and have been interpreted in terms of different degrees of binding of the mirror nuclei and in the context of the recent observations of suppression of spectroscopic strength as a function of nuclear binding, for knockout reactions on light solid targets. Mirror energy differences (MED) have been determined between the analogue $T = 2$ states and compared with the shell model predictions. MED for this mirror pair, due to their location in the shell, are especially sensitive to excitations out of the $f_{7/2}$ shell, and present a stringent test of the shell-model prescription.

1. Introduction

The attractive strong nuclear force that acts between protons and neutrons is virtually invariant to the charge of the individual nucleons. This yields one of the fundamental concepts in nuclear physics - the concept of isospin and the resulting influence of isospin symmetry upon nuclear structure [1,2]. Isospin enables us to describe two types of fermion, the proton and neutron, as two different states of the nucleon and, in this formalism, all nucleons have isospin quantum number $t = \frac{1}{2}$ with different projections for a proton ($t_z = -\frac{1}{2}$) and for a neutron ($t_z = +\frac{1}{2}$). Moreover, the nucleus has a total isospin projection on the z-axis T_z, and the total isospin of the individual nucleons, denoted by quantum number T, is given by:

$$T_z = \sum t_z = \frac{N - Z}{2} \tag{1}$$

$$\frac{|N - Z|}{2} \leq T \leq \frac{|N + Z|}{2}. \tag{2}$$

* Corresponding authors.
E-mail addresses: rayr500@york.ac.uk (R. Yajzey), michael.bentley@york.ac.uk (M.A. Bentley).

https://doi.org/10.1016/j.physletb.2021.136757

In the absence of isospin breaking interactions, states of the same isospin, T, in a set of nuclei of the same mass number (isobaric analogue states, IAS) will be degenerate. Differences in excitation energies of IAS will result from the Coulomb interaction and from any charge-dependent components of the nucleon-nucleon interaction. These isospin non-conserving (INC) forces lift the degeneracy of analogue states, break isospin symmetry and may result in isospin mixing of the states in question (e.g. [3]).

The concept of charge symmetry of the nuclear force requires that the neutron-neutron (V_{nn}) and proton-proton (V_{pp}) interactions are identical, and any interactions where $V_{nn} \neq V_{pp}$ (e.g. arising from the Coulomb force) are known as isovector interactions. The study of mirror nuclei, with exchanged numbers of neutron and protons, is an immensely powerful method to investigate isovector phenomena and how they relate to nuclear structure more generally. Differences in excitation energies between mirror nuclei, known as mirror energy differences (MED), are given by

$$MED_J = E^*_{J,T,-T_z} - E^*_{J,T,+T_z} \quad (3)$$

where E^*_{J,T,T_z} is the excitation energy of a state with spin J, total isospin T, and isospin projection T_z. MED derive entirely from isovector effects, and there have been extensive studies into MED in the pf shell, coupled to detailed shell-model calculations – e.g. [4–9]. The developments of the shell-model calculations have enabled reliable interpretation of MED in terms of electromagnetic phenomena, of both multipole and monopole origin, which are expected to provide the largest contribution to the MED [3]. These studies have yielded detailed information on the effective isospin non-conserving interactions that break the symmetry of mirror nuclei [10]. In this work, the first identification of the excited states in the proton-rich, $T_z = -2$ nucleus ^{48}Fe is produced and compared to its well studied, stable, mirror nucleus ^{48}Ti, allowing the study of MED in this $T_z = \pm 2$ pair in the $f_{\frac{7}{2}}$ shell. The excited states of ^{48}Fe were previously unknown apart from a tentative 2^+ state at 969.5(5) keV that has been reported in one previous study populated via beta-delayed proton decay of ^{49}Ni [11]. Mirror nuclei with $A = 48$, being in the centre of an isolated $f_{\frac{7}{2}}$ shell, have a unique feature in that they are cross-conjugate nuclei in the $f_{\frac{7}{2}}$ shell as well as mirror nuclei. This, in turn, means that the MED are very sensitive to cross-shell excitations, and hence they provide an especially stringent test of the model calculations.

The method employed here is the mirrored-knockout method, first applied by Milne et al. [4], in which the proton (neutron)-rich member of the mirror pair is populated by one-neutron (one-proton) knockout respectively. In this method the two nuclides required, for the two parent beams, also constitute a mirror pair. Hence this represents a complete analogue pair of reactions. Since the spectroscopic strength for the knockout process to the excited states is expected to be "mirrored" in the two reactions, this can be used to help identify the unknown states in the proton-rich system. The mirrored-knockout approach was also motivated by the well-documented observation [12–14] that single-nucleon removal reactions on light solid targets have experimental inclusive cross sections that are suppressed, compared with eikonal direct-reaction model predictions, with a suppression that depends strongly on the asymmetry, ΔS, between the separation energies of the two types of nucleon removed. A mirror pair that are well separated in Z (such as those studied here) have very different values of ΔS and yet isospin symmetry implies that similar spectroscopic strength is expected to the two sets of analogue states. Indeed, for analogue knockout reactions to a specific pair of analogue final states, the corresponding theoretical cross sections are very similar (within $\sim$20% in the current work), despite the large difference in ΔS. Hence, a detailed comparison between experimental and predicted cross sections, both inclusive and exclusive, using mirrored knockout may help shed light on the question of suppression of spectroscopic strength, and such an analysis is presented here.

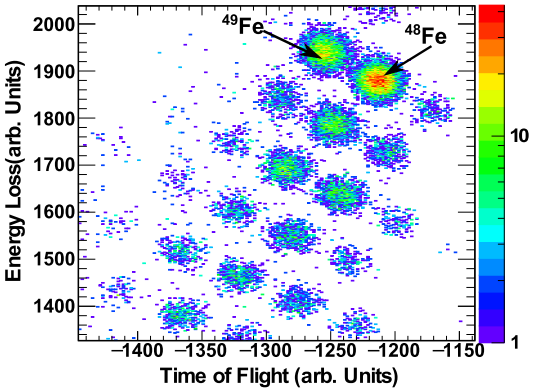

Fig. 1. The particle identification (PID) gated on the ^{49}Fe secondary beam. The plot shows the nuclei produced at the secondary target and identified through energy loss from the ionisation chamber against time of flight - see text for details.

2. Experimental details

The experiment was performed at the National Superconducting Cyclotron Laboratory (NSCL) at Michigan State University. Excited states in the mirror nuclei of interest ^{48}Fe ($T_z = -2$) and ^{48}Ti ($T_z = 2$) were populated via one-neutron and one-proton knockout from ^{49}Fe ($T_z = -\frac{3}{2}$) and ^{49}V ($T_z = +\frac{3}{2}$), respectively. The ^{58}Ni primary beam was accelerated through the K500/K1200 cyclotrons to an energy $\sim$ 160 MeV/u and fragmented on a 802 mg/cm^2 ^{9}Be production target. The resulting fragments were separated by the A1900 separator [15,16] into a cocktail beam that contained ^{49}Fe in one setting of the A1900 and ^{49}V in another. The fragment beam rates for ^{49}Fe (^{49}V) were $\sim$300 (2×10^5) particles per second, respectively, representing $\sim$0.3% (58%) of the secondary beam cocktail. These secondary beams were identified by measuring their time of flight (ToF) between two plastic scintillator detectors, one located after the A1900 fragment separator and the other in the S800 analysis beam line.

The ^{49}Fe and ^{49}V secondary beams were transported along the S800 analysis line and impinged upon a 188 mg/cm^2 ^{9}Be reaction target, from which mirrored one-nucleon knockout reactions occurred to populate states in the nuclei of interest. The post-target S800 magnet settings correspond to mid-target energies of 80 MeV/u for ^{49}Fe and 84 MeV/u for ^{49}V. The resulting reaction products were identified in the S800 by measuring the energy loss in an ionization chamber in conjunction with ToF measured between scintillators in the beam line and at the end of the S800 spectrograph, corrected using the positions and angles measured with the standard set of S800 focal plane detectors [17,18]. The resulting particle identification is demonstrated in Fig. 1, which shows that unambiguous identification of each residue can be achieved on an event-by-event basis.

The γ rays emitted from the knockout residues were identified using the Gamma-Ray Energy Tracking In-beam Nuclear Array GRETINA [19,20], consisting of nine detector modules, each comprising four high-purity germanium (HPGe) crystals. Four of these modules were centred at 58° and five centred at 90° in relation to the beam direction. In this configuration the measured photo-peak efficiency, without addback or tracking, was determined to be 6.4(1)% for a 1-MeV γ ray emitted at rest, rising to 6.7(1)% when moving at $v/c \sim 0.4$, as in the current work. To maximise photo-peak efficiency and optimise the $\gamma - \gamma$ coincidence analysis, an add-back procedure was applied in which energies deposited in neighbouring GRETINA crystals were summed. This add-back procedure, which was used rather than a full gamma-ray track-

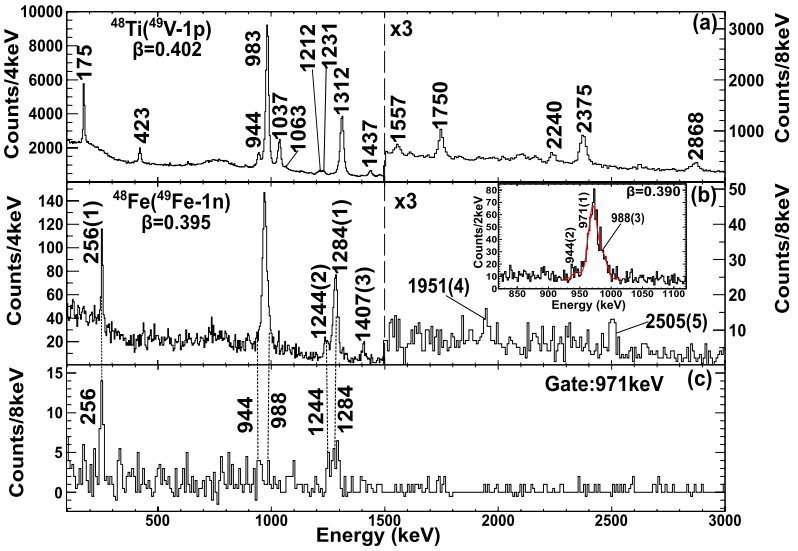

Fig. 2. The Doppler corrected spectra, using an add-back procedure (see text), for (a) ^{48}Ti and (b) ^{48}Fe identified following one-nucleon knockout from ^{49}V and ^{49}Fe. The $\beta = v/c$ value in (a) and (b) is optimised for fast transitions and a lower β is used for the spectrum insert of (b) for the 971-keV transition (see text). The spectrum used in the insert in (b) was produced without add-back applied, since fits used in the analysis were only applied to spectra without add-back. All the fits applied were Gaussian. (c) A spectrum from a γ-γ coincidence analysis, using add-back, measured to be in coincidence with the 971-keV transition in ^{48}Fe.

ing algorithm (e.g. see [19]), was not applied when determining efficiency-corrected γ-ray intensities. In the case of one-nucleon knockout from the $J^\pi = \frac{7}{2}^-$ ground states of the ^{49}Fe and ^{49}V secondary beams to ^{48}Fe and ^{48}Ti, positive-parity states up to $J^\pi = 6^+$ can be populated directly through knockout from the pf-shell orbitals near the Fermi level. Similarly, knockout from the more bound sd-shell levels can populate negative-parity states up to 6^-.

3. Results

The Doppler-corrected γ-ray spectra of ^{48}Fe and ^{48}Ti are shown in Figs. 2(a) and 2(b) respectively. The angle for the Doppler correction was determined from the recorded position, determined by pulse-shape analysis, of the highest-energy interaction for that gamma-ray event (see [19]). For a fast transition, in this experiment, the best energy resolution achieved was around 1.4% (FWHM) for 1-MeV γ ray. The optimum recoil velocity, $\beta = v/c$, used for the Doppler correction, was determined by varying β until any angular dependence of the observed γ-ray energy was removed. This can depend on the effective lifetime of the states emitting the γ ray (and of the states feeding them) since fast decays that occur on sub-ps timescales will decay near the centre of the target, whilst longer-lived states of the order of > 10 ps will decay outside the target, with a lower recoil velocity. Values of β = 0.402 and 0.395 were found to optimise the Doppler correction for the majority of peaks seen in Figs. 2(a) and 2(b), most of which (in the known case, ^{48}Ti) decay from short-lived states with lifetimes of < 1 ps. However, a lower recoil velocity was needed to optimise the two largest transitions of 983 keV in ^{48}Ti and 971 keV in ^{48}Fe. This is consistent with the fact that the 983-keV, $J^\pi = 2_1^+$ state in ^{48}Ti is known to have a longer half-life of ~ 4 ps [21], and hence the analogue transition in ^{48}Fe is likely to have a similar half life. This is demonstrated in the inset to Fig. 2(b) which shows the spectrum created using β = 0.390, optimised for the 971(1)-keV transition.

To identify excited states in ^{48}Fe from one-neutron knockout from ^{49}Fe, we first examine the analogue reaction – one-proton knockout from ^{49}V to ^{48}Ti – since, structurally, the reaction processes are expected to be very similar. The observed spectrum for ^{48}Ti, Fig. 2(a), is dominated by the γ-ray transitions from positive-parity states with $J^\pi = 2^+, 4^+$, and 6^+ – with two states of each J^π observed. These states can all be populated directly from one-nucleon knockout from the $\frac{7}{2}^-$ ground state of the ^{49}V secondary beam. Although $J^\pi = 6^+$ is the maximum spin that can be populated directly in knockout from the pf-shell, there is weak evidence for decay from the 8^+ state, presumably populated indirectly through unobserved decays from higher-lying states (see later discussion). The negative-parity states, observed in this work, can be populated directly through knockout from any of the more-bound sd orbitals. The level scheme containing γ rays observed in ^{48}Ti is shown in the right panel of Fig. 3. All the labelled γ-ray transitions observed in Fig. 2(a) have been previously assigned to ^{48}Ti [21], and all the energies measured here are consistent with those of Ref. [21]. The more precise energies from Ref. [21] are used in Figs. 2(a) and 3.

Fig. 2(b) shows γ rays from excited states of the highly proton-rich nucleus ^{48}Fe, which have been unambiguously observed for the first time in this work. Uncertainties on the newly-identified γ-ray energies comprise statistical and systematic errors, the latter associated with uncertainties in β and the effective target position. The only transition previously assigned to ^{48}Fe is a 969.5(5) transition observed following beta decay of ^{49}Ni [11]. This transition was weak (4-5 counts observed) but tentatively assigned as the $2^+ \rightarrow 0^+$ transition in ^{48}Fe populated through beta-delayed proton emission. This transition is confirmed in the current work as 971(1) keV. With the high energy resolution of GRETINA, and the lower velocity applied for the Doppler correction (see inset to Fig. 2(b)), three close-lying transitions in ^{48}Fe are observed corresponding to 944(2), 971(1), and 988(3) keV - the latter of which appears as a tail on the right of the 971-keV peak. Comparison of the γ-ray energies and intensities with ^{48}Ti leads to the conclusion that the isobaric analogue states with $J^\pi = 2^+$, 4^+ and 6^+ are populated in both reactions.

The observed transitions have been placed, in the current work, in a new level scheme for ^{48}Fe in the left panel of Fig. 3. The ordering of the γ-ray transitions was initially made on the basis of mirror symmetry arguments (the analogue knockout reactions and the γ-ray energy similarities) and intensity arguments. For the strongest transitions, this was confirmed by a γ-γ coincidence analysis afforded by the excellent in-beam resolution and efficiency of GRETINA. An example, in Fig. 2(c), is the γ-ray spectrum mea-

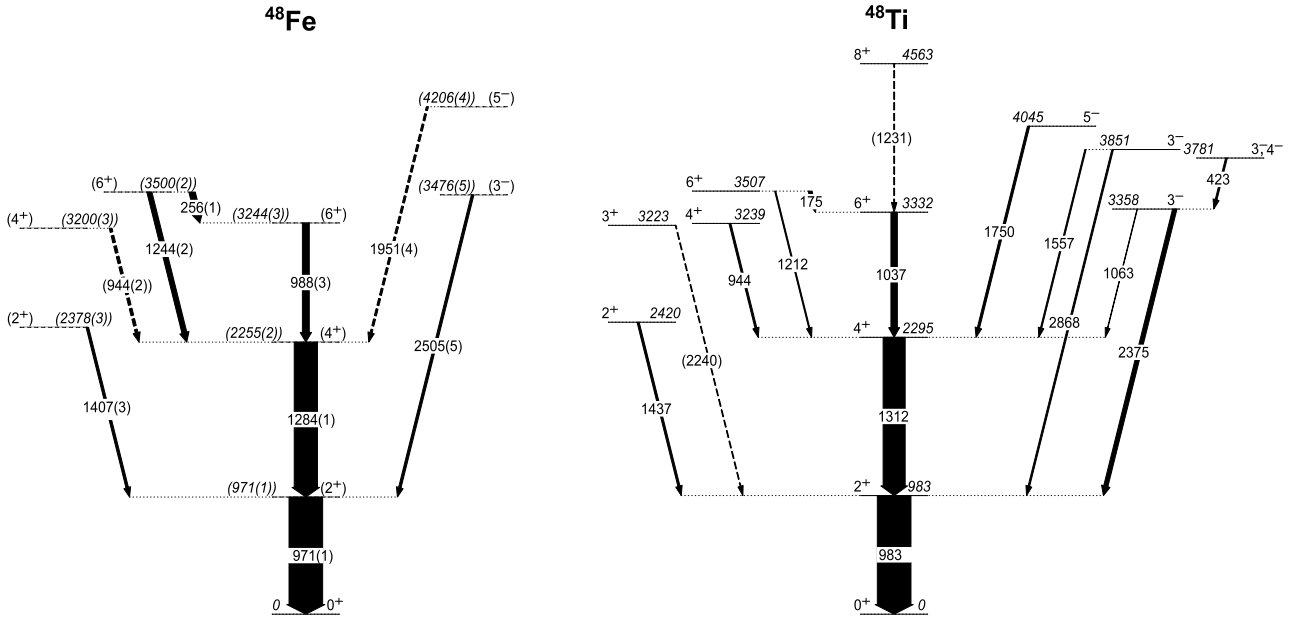

Fig. 3. The energy level scheme for ^{48}Fe deduced from the current work compared with the level scheme of ^{48}Ti as observed in this experiment. The intensities of the γ rays are indicated by the width of the arrows and are determined relative to the intensity of the $2_1^+ \rightarrow 0^+$ transition. The dashed lines indicate tentative transitions.

Table 1
The experimental and theoretical exclusive cross sections for states directly populated in this work through one-nucleon knockout - see text for details. The inclusive cross sections are listed in the final row (the theoretical inclusive cross section could not be determined for ^{48}Ti - see text). The theoretical cross sections are calculated using the experimental separation- and residue-excitation energies.

J_i^π	^{48}Fe		^{48}Ti	
	σ_{exp}(mb)	σ_{th}(mb)	σ_{exp}(mb)	σ_{th}(mb)
0^+	3(2)	5.49	18(3)	6.68
2_1^+	0.9(9)	0.29	4(2)	0.34
4_1^+	1.1(8)	3.59	13(2)	4.40
2_2^+	0.4(2)	3.69	3.2(4)	4.28
3_1^+			1.2(3)	0.38
4_2^+	0.5(4)	1.85	2.8(4)	2.20
6_1^+	0.1(6)	1.21	8.3(9)	1.43
3_1^-	0.4(2)		4.6(6)	
6_2^+	1.9(4)	6.83	7.2(7)	8.10
$3_2^-, 4_1^-$			2.5(3)	
3_3^-			4.2(6)	
5_1^-	0.3(2)		3.4(4)	
8_1^+			1.4(4)	
inclusive	8(2)	22.9	74(6)	-

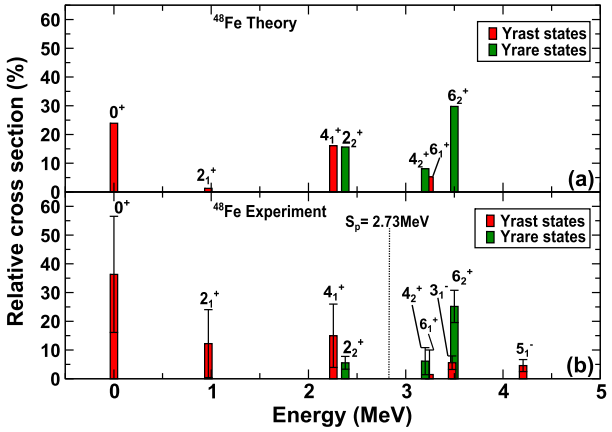

Fig. 4. (a) Calculated and (b) experimental relative cross sections for excited states in ^{48}Fe resulting from one-neutron knockout from ^{49}Fe ground state $7/2^-$. The sum of the statistical and systematic uncertainties are given. Since the model-space used for (a) is restricted to positive-parity states, the total experimental cross section used for (b) is the total for the positive-parity states only.

sured in coincidence with the 971(1) keV ($2_1^+ \rightarrow 0^+$) transition, which shows the expected γ-ray transitions in coincidence with this transition. The spins and parities for ^{48}Fe states were assigned through mirror symmetry arguments only. The placement of some of the transitions in this scheme is tentative (e.g. low statistics, where coincidence measurements are not possible or where there are large shifts in the analogue γ-ray energies). These are indicated by dashed lines in Fig. 3. Of particular note here is the observation that, for the excited positive-parity states, the knock-out process populates both the lowest-energy states of each J ($J^\pi = 2_1^+$, 4_1^+ and 6_1^+ – the *yrast* states) and the next lowest-energy states for that J ($J^\pi = 2_2^+$, 4_2^+ and 6_2^+ – the *yrare* states). There is also evidence for the population of the analogue states of the negative-parity states observed in ^{48}Ti. The widths of the arrows in Fig. 3 are proportional to the relative intensity of the γ-ray transitions.

The experimental cross sections, both inclusive σ_{inc} (summed over all states) and exclusive σ_{excl} (each individual state) have been determined for both members of the mirror pair, using measured particle intensities, efficiency-corrected γ-ray intensities and observed γ-ray feeding. For ^{49}Fe to ^{48}Fe an inclusive cross section of 8.4 ± 0.2(stat.) ± 1.5(sys.) mb was determined and exclusive cross sections are listed in Table 1. Fig. 4(b) shows the relative cross section for each state ($\sigma_{excl}/\sigma_{inc}$) for excited states in ^{48}Fe. The strong direct population of the yrare states is evident. To interpret these observations, one-nucleon knockout cross sections were calculated using a combination of the eikonal reaction dynamics e.g. [22] and shell-model calculations. The single nucleon removal wavefunctions were calculated in Wood-Saxon plus spin-orbit potentials with geometries constrained using Hartree-Fock calculations [12]. Full-*pf* shell-model calculations using the KB3G [23] interaction in the ANTOINE code [24] were employed to compute the spec-

troscopic factors. Only positive-parity states are accessible in this model due to the shell-model space used. The predicted exclusive cross sections are listed in Table 1 and the theoretical inclusive cross section is 22.9 mb. Here we define the latter as the sum of theoretical cross sections for all bound states in the shell-model plus the theoretical cross sections for those states observed above the proton separation energy. The relative theoretical cross sections are shown in Fig. 4(a) and can be directly compared with the experimental data in Fig. 4(b). Though the absolute values of the measured exclusive cross sections are generally much smaller than the theoretical values, there is good agreement between the distribution of relative cross sections, and some of the key observations of the experimental data (e.g. strong direct population of the yrare states) is well reproduced.

The strong suppression of experimental cross sections, compared with the presented model predictions, for one-nucleon knockout at intermediate energies has been the subject of a number of recent studies [12–14]. In that work, it was show that the observed suppression depends strongly on the (a)symmetry of the separation energies of the two nucleon species. This was denoted ΔS – defined as $S_p - S_n$ for proton removal and $S_n - S_p$ for neutron removal. It was found that for removal of strongly-bound particles from weakly-bound systems (e.g. neutron-removal from nuclei near the proton-drip line, as in the current work) the suppression was strong with R_S ($=\sigma_{exp}/\sigma_{th}$) reducing from ~0.6(1) to ~0.3(1) for positive values of ΔS from 0 to 20 MeV [14]. Using an effective value of S_n, taking the excitation energies of the final states into account (see [13] for details), the one-neutron removal reactions to ^{48}Fe correspond to $\Delta S = 14.3$ MeV, and the inclusive cross section suggests a value of R_S of 0.36(6), consistent with the observations of reference [13]. Indeed, in the current work, there is also evidence of removal of *sd*-shell nucleons (approximately 10% of the total cross section), which are excluded from the shell-model calculation. This suggests a modest underestimate of the theoretical inclusive cross section, which would reduce R_S further.

As a starting point, the mirrored reaction, proton removal from ^{49}V to ^{48}Ti, might be expected to present similar results, due to isospin symmetry - e.g. the spectroscopic factors for specific knockout paths are expected to be close to identical. Indeed inspection of the level schemes, and relative intensities, in Fig. 3 indicates a similar population pattern. However, the experimental inclusive cross section for ^{49}V to ^{48}Ti was measured to be 74.4 ± 0.4(stat.) ± 6.2(sys.) mb, a factor of ~ 9 times larger than the analogue reaction to ^{48}Fe. In this more bound system, it is not possible to precisely determine a theoretical inclusive cross section using the usual method [12,13] since the high separation energies of the ^{48}Ti residual nucleus make a shell-model calculation of all bound final states impracticable.

Two other examples of analogue cross-section measurements in mirrored-knockout reactions appear in the literature [25,26] and in both cases the inclusive cross sections were also asymmetric, although not to the extent observed here. Wimmer et al. [25] observed about a factor of ~ 4 difference in the inclusive cross sections for mirrored one-nucleon knockout to the $T = 1$, $A = 70$ mirror pair and Spieker et al. [26] a factor of ~ 3 difference for mirrored one-nucleon knockout to the $T = \frac{1}{2}$, $A = 55$ mirror pair. In both these cases, the authors suggest that the asymmetry may be, in part, due to the different binding of the mirror nuclei. For ^{48}Fe, the nucleon separation energies are indeed highly asymmetric – the most recent mass evaluations [27] (which include the recent mass measurement of ^{48}Fe [28]) yield separation energies of $S_p = 2.73$ MeV, $S_n = 18.95$ MeV compared with $S_p = 11.4$ MeV, $S_n = 11.6$ MeV for ^{48}Ti. Thus, one may expect population of highly-excited ^{48}Ti bound states, the analogue states of which, in ^{48}Fe, are unbound and decay by proton emission - hence are excluded from the measurement. Our analysis indicates that removal of *sd*-shell particles is likely to play a significant role. Hartree-Fock calculations using the SkX Skyrme interaction [29] indicate that, for ^{49}V (the beam used for proton-removal to ^{48}Ti), the *sd*-shell proton orbitals are about 5.0 MeV ($d_{3/2}$), 5.3 MeV ($s_{1/2}$) and 9.8 MeV ($d_{5/2}$) more bound than the $f_{7/2}$ protons at the Fermi level. Hence these provide reasonable estimates for the excitation-energy centroids, in ^{48}Ti, for *sd*-shell proton removal. The majority of this *sd*-shell knockout strength would therefore populate bound states in ^{48}Ti ($E^* < 12$ MeV) and unbound states ($E^* > 3$ MeV) for the analogue neutron-removal reactions to ^{48}Fe. In this interpretation, therefore, the large asymmetry observed in the inclusive cross sections is most likely due to this ~ 9-MeV difference, between ^{48}Ti and ^{48}Fe, in the excitation-energy range over which bound states exist. It is instructive to estimate a theoretical (maximum) inclusive cross section to ^{48}Ti through evaluating the sum-rule strength for removal of $f_{7/2}$- and *sd*-shell protons (i.e. those at, and below, the Fermi level) the centroids of which are all expected to be bound for ^{48}Ti. In this estimate, the average excitation energies of the states populated by *sd*-shell knockout are taken to be the above centroid estimates. The included *pf* shell-model states, to $E^* = 3.5$ MeV, account for a summed spectroscopic strength of 2.4. The remaining 0.6 units, to states at higher energy, can account for a maximum additional cross section of less than 6 mb, given the calculated *pf*-shell orbital cross sections. Adding removals from the assumed-filled *sd*-shell orbitals then yields a maximum (sum-rule) inclusive cross section of ~ 140 mb. This, coupled to the anticipated degree of suppression of ~0.6(1) estimated from Ref. [14], provides a reasonable account of the experimental cross section of 74(6) mb.

If this interpretation is correct, there must be significant *unseen* feeding into the low-lying yrast states and ground state of ^{48}Ti, since states along the yrast line would be expected to gather intensity from statistical feeding from higher-energy states. Indeed, the large observed cross section to the ^{48}Ti ground state, compared with the smaller theoretical prediction, suggests additional unseen feeding. Conversely, the yrare states, which are predicted to have strong *direct* population in this particular case, might be expected to be less susceptible to this indirect feeding. For example, we note that in fusion-evaporation reactions populating ^{48}Ti (e.g. [30]), in which low-spins states are fed indirectly through statistical feeding, the 2_2^+ and 4_2^+ states (which lie ~ 1 MeV above the yrast line) receive no population at all. Comparison of the exclusive cross sections for these analogue yrare states (see Table 1) shows that a significant cross-section asymmetry remains and which is consistent in magnitude for all three pairs of yrare states. The experimental (exclusive) cross sections to these states are ~ 5 times higher, on average, in ^{48}Ti than in ^{48}Fe. It should be noted that we cannot rule out further indirect feeding for these states, especially ^{48}Ti, and hence these exclusive cross sections should be regarded as upper limits.

The systematics of $R_S = \sigma_{exp}(\text{inc})/\sigma_{th}(\text{inc})$ as a function of ΔS, see Tostevin and Gade [13], have some intriguing potential consequences for mirrored knockout reactions of the kind presented here. The R_S data gathered in that systematic analysis correspond to inclusive cross sections only. However, if the trend of the R_S plot is also observed for analogue (i.e. mirrored) exclusive cross sections, this could only arise if the experimental cross sections were significantly larger in the well-bound nucleus compared with its weakly-bound mirror partner, despite the presumed analogue nature of the knockout process – in qualitative agreement with our tentative observations here. This is because (a) the mirrored reactions are well separated in ΔS (e.g. ~16 MeV difference in this case), (b) the theoretical spectroscopic factors for the knockout paths in the shell model are essentially identical, and (c) the theoretical single-particle cross sections for in the reaction model used do not have a strong ΔS-dependence (~ 20% in this case).

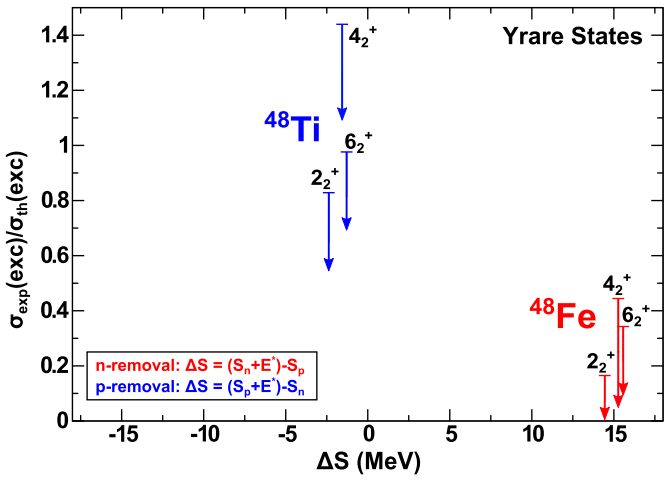

Fig. 5. The ratio of the experiential to the theoretical cross sections for yrare states 2_2^+, 4_2^+ and 6_2^+ plotted as a function of the separation energies ΔS for both one neutron removal from ^{49}Fe to ^{48}Fe (red) and for one proton removal from ^{49}V to ^{48}Ti (blue).

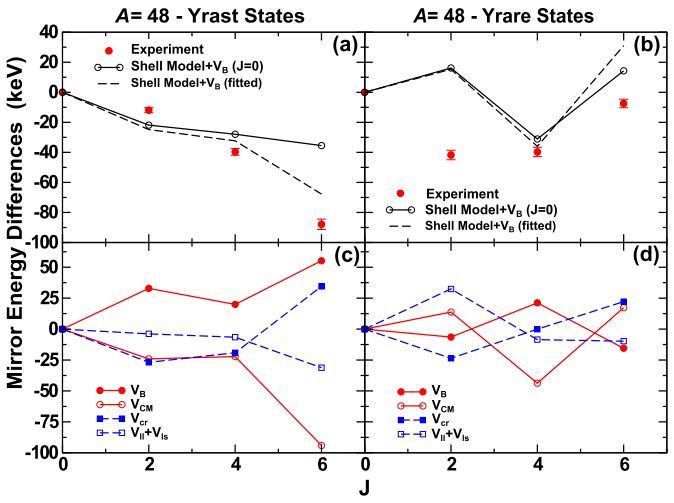

Fig. 6. The experimental and theoretical MED for the A=48, T_z = ±2 mirror yrast states (left) and yrare states (right). In (a) and (b) the two theoretical lines correspond to two different ways for defining the INC term V_B. The solid line and the dashed line both are the shell-model calculations which include all the four components, where the solid line uses single −100 keV INC matrix element for J=0 for all fp-orbitals, and the dashed uses four parameters extracted from the fit across the $f_{\frac{7}{2}}$ shell [31]. (c) and (d) show the four components of the shell-model calculations (defined in the text): the sum of the four components gives in solid lines in (a) and (b). The MED for the $J \neq 0$ yrare states in (b) and (d) are plotted relative the $J = 0$ ground state.

Fig. 5 shows the ratio of the experimental and theoretical exclusive cross sections for these three pairs of yrare analogue states $\sigma_{exp}(\text{exc})/\sigma_{th}(\text{exc})$ as a function of ΔS. It is interesting to note that the degree of suppression (experiment compared with theory) has a similar trend to the published R_S systematics for inclusive cross sections. Although the absolute values of the ratios presented in Fig. 5 for exclusive cross sections will be sensitive to the shell-model calculations for individual states, the trend with ΔS should not be significantly affected as the mirror reactions probe the same spectroscopic factors.

Experimental mirror energy differences (MED) were extracted through comparison of the excitation energies for the analogue states in the mirror nuclei ^{48}Fe and ^{48}Ti. As well as the large difference in Z between the nuclei, this mirror pair has two other apparently unique features. Firstly, in both mirror nuclei, for all the positive parity states observed, both the yrast and yrare states are populated allowing, unusually, an MED analysis of both types of state. Secondly, this pair, having 48 particles (exactly midway through the $f_{\frac{7}{2}}$ shell) has a cross-conjugate symmetry as well as mirror symmetry. Considering the approximation of an isolated $f_{\frac{7}{2}}$ shell, ^{48}Fe has two neutrons and two proton holes, whilst ^{48}Ti has two protons and two neutron holes. In this scenario, all multipole Coulomb effects that contribute to the MED (which normally dominate) would be zero. Since wave functions of the form $\pi(\nu)f_{\frac{7}{2}}^6\nu(\pi)f_{\frac{7}{2}}^2$ will be large, the Coulomb multipole contributions to the MED may be expected to be small.

The experimental and predicted MED are presented for the yrast and yrare states in Figs. 6(a) and (b) respectively. The MED can be interpreted by large-scale shell-model calculations, using the full fp space implemented using the ANTOINE code [24]. The shell-model method used is based on the prescription of Refs. [3,10] which accounts for multipole and monopole contributions to the MED of Coulomb and magnetic origin. Four contributions to the MED are calculated within the shell model. The Coulomb multipole contribution, (V_{CM}), accounts for the Coulomb effect of recoupling angular momenta of pairs of protons, achieved through adding the Coulomb two-body interaction to the nuclear residual interaction. The radial contribution (V_{Cr}) is the monopole Coulomb contribution associated with changes in the nuclear radius with J, calculated as explained in Ref. [10]. Shifts in the shell-model single-particle energy levels due to Coulomb and magnetic effects (V_{ll}+V_{ls}) are included according to the method of Zuker [3]. The final term is an empirical isovector, $V_{pp} - V_{nn}$, contribution which was found to be necessary in addition to V_{CM} [3]. This isospin non-conserving contribution V_B was shown [31] to be strongly dependent on the angular-momentum coupling of nucleon pairs. The origin of the V_B term is presently unclear and a discussion of this is provided in Refs. [10,31].

A comparison between the experimental MED and the shell-model calculations is shown in Fig. 6(a) for the yrast states and Fig. 6(b) for the yrare states. The solid black lines in Figs. 6(a) and (b) is the shell-model calculation and the four individual components for this calculation are shown in Figs. 6(c) and (d). Despite the cross-conjugate nature of the mirror pair, the magnitude of the experimental MED is large, comparable with other cases in this region [10], and the multipole components of the MED in the shell model are the dominant components. For the shell-model calculations, a single matrix element for V_B of −100 keV for $J = 0$ couplings is included (i.e. added directly to the shell-model matrix element for protons). It was shown in reference [31] that the $J = 0$ coupling is by far the most important contribution to V_B, and a best fit value of -79 keV was extracted. The $J = 0$ dominance suggests that a monopole pairing effect is at the heart of this empirical phenomenon. Moreover, for energy differences between excited states of isospin triplets [32], a single isotensor matrix element for $J = 0$ (in that case +100 keV) was found to provide an excellent description of triplet energy differences across the pf shell. Hence an isovector component of −100 keV for $J = 0$ is used for V_B in the solid lines in Fig. 6.

The negative trend of the MED for the yrast states is reproduced in the calculations, with good agreement for the 2_1^+ and 4_1^+ states, although the calculations diverge from experiment for the yrast 6_1^+ state. The inclusion of the V_B term does not, in this case, yield as dramatic an improvement in the agreement as in other cases in the region [31]. Switching off the V_B term improves the agreement for the 6_1^+ state and significantly worsens it for the 2_1^+ state. For the yrare states, the 2_2^+ state is not well reproduced by the calculations, with or without V_B, with better agreement for the 4_2^+ and 6_2^+ states. The inconsistent agreement between experiment and model may be attributed to the inadequacy of the fp space - especially for protons (neutrons) in ^{48}Ti (^{48}Fe):

there are only two such particles in the fp shell-model space. A similarly poor agreement was found for the $A = 46, T = 1$ mirrors [10], for presumably similar reasons (i.e. missing two-particle two-hole excitations across the ^{40}Ca shell closure). For comparison, the shell-model calculations were repeated in full using the other common pf-shell interaction, GXPF1A [33], used more widely in the upper pf shell. The MED results are very similar, and the agreement between the model and experiment for the 6_1^+ and 2_2^+ state is not improved. It is interesting to note that, because of the cross-conjugate symmetry described earlier for this $A = 48$ mirror pair, all non-zero multipole contributions to the MED must derive from excitations out of the $f_{\frac{7}{2}}$ shell. Indeed, in the shell-model prescription used here, all four components derive solely from excitations out of the $f_{\frac{7}{2}}$ shell, and are all zero when such excitations are forbidden. The exclusion, in these calculations, of *sd* excitations across the ^{40}Ca shell closure is therefore likely to undermine the ability of the model to correctly reproduce the data. This mirror pair is clearly a good test case for any shell-model approach that is capable of a calculation in a space that contains the lower-pf and upper-*sd*-shell orbitals. In Ref. [31] a detailed analysis of the isospin-non-conserving term V_B was performed, where it was shown that the V_B matrix elements, required to account for the experimental data, were strongly angular-momentum dependent. Although a single, negative, $J = 0$ matrix element is largely sufficient to account for the data, a better overall fit was obtained for four matrix elements of -72, +32,+8,-12 keV for J= 0, 2, 4, 6 couplings, respectively, of the $f_{\frac{7}{2}}$ orbital. A shell-model calculation using these coefficients for V_B is shown by the dashed line in Figs. 6(a) and (b) and it is noteworthy that this enables a better overall agreement for the yrast states.

4. Conclusion

In summary, a new level scheme has been established for the proton-rich nucleus ^{48}Fe through application of the mirrored-knockout approach. Significant differences were observed between the inclusive knockout reaction cross sections for the mirrored reactions. The difference between nucleon separation energies for the mirrors, leading to very different degrees of *sd*-shell knockout strength to bound states, is likely to be the dominant reason for this observation. Experimental exclusive cross sections were also compared for some specific pairs of analogue states (yrare states), where isospin symmetry suggests that the cross sections should be similar. Although significant differences in these cross sections were tentatively suggested by the data, additional unseen feeding to the states cannot be ruled out and the cross sections were presented as upper limits. Since the two members of the mirror pair have very different degrees of binding, the mirrored exclusive cross sections were discussed in the context of the well-documented systematic suppression of spectroscopic strength, as a function of binding energy, for knockout reactions at intermediate energies. Mirror energy differences for this $T = 2$ mirror pair were analysed in the context of a shell-model calculation including isospin-non-conserving contributions. Due to the additional cross-conjugate symmetry of these $A = 48$ mirror nuclei, the MED are shown to be especially sensitive to cross-shell excitations and hence probe the validity of the shell-model space used.

Declaration of competing interest

The authors declare that they have no known competing financial interests or personal relationships that could have appeared to influence the work reported in this paper.

Acknowledgements

Discussions with M. Spieker on data analysis are gratefully acknowledged. RY acknowledges financial support for a PhD studentship from Jazan University, Saudi Arabia. TH, SU, DK and S-JL acknowledge support from the UKRI Science and Technology Facilities Council (STFC). This work is supported by STFC under grant numbers ST/L005727/1 and ST/P003885/1. The work was supported by the National Science Foundation (NSF) under PHY-1565546 and by the US Department of Energy (DOE), Office of Science, Office of Nuclear Physics under Grant No. DE-SC0020451. GRETINA was funded by the DOE, Office of Science. Operation of the array at NSCL was supported by the DOE under Grant Nos. DE-SC0014537 (NSCL)and DE-AC02-05CH11231(LBNL).

References

[1] E. Wigner, On the consequences of the symmetry of the nuclear Hamiltonian on the spectroscopy of nuclei, Phys. Rev. 51 (2) (1937) 106.
[2] R. Machleidt, I. Slaus, The nucleon-nucleon interaction, J. Phys. G, Nucl. Part. Phys. 27 (5) (2001) R69.
[3] A.P. Zuker, S.M. Lenzi, G. Martinez-Pinedo, A. Poves, Isobaric multiplet yrast energies and isospin nonconserving forces, Phys. Rev. Lett. 89 (14) (2002) 142502.
[4] S.A. Milne, M.A. Bentley, E.C. Simpson, P. Dodsworth, T. Baugher, D. Bazin, J.S. Berryman, A.M. Bruce, P.J. Davies, C.Aa. Diget, et al., Mirrored one-nucleon knockout reactions to the $T_z = \pm 3/2$, A = 53 mirror nuclei, Phys. Rev. C 93 (2) (2016) 024318.
[5] J. Ekman, C. Fahlander, D. Rudolph, Mirror symmetry in the upper fp shell, Mod. Phys. Lett. A 20 (39) (2005) 2977–2992.
[6] K. Kaneko, Y. Sun, T. Mizusaki, S. Tazaki, Variation in displacement energies due to isospin-nonconserving forces, Phys. Rev. Lett. 110 (17) (2013) 172505.
[7] K. Kaneko, S. Tazaki, T. Mizusaki, Y. Sun, M. Hasegawa, G.De. Angelis, Isospin symmetry breaking at high spins in the mirror pair ^{67}Se and ^{67}As, Phys. Rev. C 82 (6) (2010) 061301.
[8] M.J. Taylor, M.A. Bentley, J.R. Brown, P.E. Kent, R. Wadsworth, C.J. Lister, D. Seweryniak, M.P. Carpenter, R.V.F. Janssens, S. Zhu, et al., Isospin symmetry in the odd-odd mirror nuclei ^{44}V/^{44}Sc, Phys. Rev. C 84 (6) (2011) 064319.
[9] P.J. Davies, M.A. Bentley, T.W. Henry, E.C. Simpson, A. Gade, S.M. Lenzi, T. Baugher, D. Bazin, J.S. Berryman, A.M. Bruce, et al., Mirror energy differences at large isospin studied through direct two-nucleon knockout, Phys. Rev. Lett. 111 (7) (2013) 072501.
[10] M.A. Bentley, S.M. Lenzi, Coulomb energy differences between high-spin states in isobaric multiplets, Prog. Part. Nucl. Phys. 59 (2) (2007) 497–561.
[11] C. Dossat, N. Adimi, F. Aksouh, F. Becker, A. Bey, B. Blank, C. Borcea, R. Borcea, A. Boston, M. Caamano, et al., The decay of proton-rich nuclei in the mass A = 36–56 region, Nucl. Phys. A 792 (1–2) (2007) 18–86.
[12] A. Gade, P. Adrich, D. Bazin, M.D. Bowen, B.A. Brown, C.M. Campbell, J.M. Cook, T. Glasmacher, P.G. Hansen, K. Hosier, et al., Reduction of spectroscopic strength: weakly-bound and strongly-bound single-particle states studied using one-nucleon knockout reactions, Phys. Rev. C 77 (4) (2008) 044306.
[13] J.A. Tostevin, A. Gade, Systematics of intermediate-energy single-nucleon removal cross sections, Phys. Rev. C 90 (5) (2014) 057602.
[14] J.A. Tostevin, A. Gade, Updated systematics of intermediate-energy single-nucleon removal cross sections, Phys. Rev. C 103 (2021) 054610.
[15] D.J. Morrissey, et al., A new high-resolution separator for high-intensity secondary beams, Nucl. Instrum. Methods Phys. Res., Sect. B, Beam Interact. Mater. Atoms 126 (1–4) (1997) 316–319.
[16] D.J. Morrissey, B.M. Sherrill, M. Steiner, A. Stolz, I. Wiedenhoever, Commissioning the A1900 projectile fragment separator, Nucl. Instrum. Methods Phys. Res., Sect. B, Beam Interact. Mater. Atoms 204 (2003) 90–96.
[17] D. Bazin, J.A. Caggiano, B.M. Sherrill, J. Yurkon, A. Zeller, The S800 spectrograph, Nucl. Instrum. Methods Phys. Res., Sect. B, Beam Interact. Mater. Atoms 204 (2003) 629–633.
[18] J. Yurkon, D. Bazin, W. Benenson, D.J. Morrissey, B.M. Sherrill, D. Swan, R. Swanson, Focal plane detector for the S800 high-resolution spectrometer, Nucl. Instrum. Methods Phys. Res., Sect. A, Accel. Spectrom. Detect. Assoc. Equip. 422 (1–3) (1999) 291–295.
[19] D. Weisshaar, D. Bazin, P.C. Bender, C.M. Campbell, F. Recchia, V. Bader, T. Baugher, J. Belarge, M.P. Carpenter, H.L. Crawford, et al., The performance of the γ-ray tracking array GRETINA for γ-ray spectroscopy with fast beams of rare isotopes, Nucl. Instrum. Methods Phys. Res., Sect. A, Accel. Spectrom. Detect. Assoc. Equip. 847 (2017) 187–198.
[20] S. Paschalis, I.Y. Lee, A.O. Macchiavelli, C.M. Campbell, M. Cromaz, S. Gros, J. Pavan, J. Qian, R.M. Clark, H.L. Crawford, et al., The performance of the gamma-ray energy tracking in-beam nuclear array gretina, Nucl. Instrum. Methods Phys. Res., Sect. A, Accel. Spectrom. Detect. Assoc. Equip. 709 (2013) 44–55.

[21] T.W. Burrows, Nuclear data sheets for A = 48, Nucl. Data Sheets 107 (7) (2006) 1747–1922.
[22] P.G. Hansen, J.A. Tostevin, Direct reactions with exotic nuclei, Annu. Rev. Nucl. Part. Sci. 53 (1) (2003) 219–261.
[23] A. Poves, J. Sanchez Solano, E. Caurier, F. Nowacki, Shell model study of the isobaric chains A = 50, A = 51 and A = 52, Nucl. Phys. A 694 (1) (2001) 157–198.
[24] E. Caurier, F. Nowacki, Acta Phys. Pol. B 30 (1999) 705.
[25] K. Wimmer, W. Korten, T. Arici, P. Doornenbal, P. Aguilera, A. Algora, T. Ando, H. Baba, B. Blank, A. Boso, et al., Shape coexistence and isospin symmetry in A = 70 nuclei: spectroscopy of the $T_z = -1$ nucleus ^{70}kr, Phys. Lett. B 785 (2018) 441–446.
[26] M. Spieker, A. Gade, D. Weisshaar, B.A. Brown, J.A. Tostevin, B. Longfellow, P. Adrich, D. Bazin, M.A. Bentley, J.R. Brown, et al., One-proton and one-neutron knockout reactions from N = Z = 28 ^{56}Ni to the A = 55 mirror pair ^{55}Co and ^{55}Ni, Phys. Rev. C 99 (5) (2019) 051304.
[27] W. Meng, W.J. Huang, F.G. Kondev, G. Audi, S. Naimi, The ame 2020 atomic mass evaluation (ii). Tables, graphs and references, Chin. Phys. C 45 (3) (2021) 030003.
[28] C.Y. Fu, Y.H. Zhang, M. Wang, X.H. Zhou, Yu.A. Litvinov, K. Blaum, H.S. Xu, X. Xu, P. Shuai, et al., Mass measurements for the $T_z = -2$ fp-shell nuclei ^{40}Ti, ^{44}Cr, ^{46}Mn, ^{48}Fe, ^{50}Co, and ^{52}Ni, Phys. Rev. C 102 (Nov 2020) 054311.
[29] B. Alex Brown, New Skyrme interaction for normal and exotic nuclei, Phys. Rev. C 58 (1) (1998) 220.
[30] E.K. Warburton, C.W. Beausang, D.B. Fossan, L. Hildingsson, W.F. Piel, J.A. Becker, High-spin $(f_{7/2})^{A-40}$ states in ^{47}Ti, ^{47}Sc, ^{44}Ca, ^{45}Ca, and ^{48}Ti via ^{36}C fusion-evaporation reactions, Phys. Rev. C 34 (1986) 136–151.
[31] M.A. Bentley, S.M. Lenzi, S.A. Simpson, C.Aa. Diget, Isospin-breaking interactions studied through mirror energy differences, Phys. Rev. C 92 (2) (2015) 024310.
[32] S.M. Lenzi, M.A. Bentley, R. Lau, C.Aa. Diget, Isospin-symmetry breaking corrections for the description of triplet energy differences, Phys. Rev. C 98 (5) (2018) 054322.
[33] M. Honma, T. Otsuka, B.A. Brown, T. Mizusaki, Shell-model description of neutron-rich pf-shell nuclei with a new effective interaction gxpf 1, Eur. Phys. J. A 25 (2005) 09.